NJC

ROYAL SOCIETY OF CHEMISTRY

PAPER

View Article Online
View Journal

Cite this: DOI: 10.1039/d1nj01506k

Prussian blue-doped PAMAM dendrimer nanospheres for electrochemical immunoassay of human plasma cardiac troponin I without enzymatic amplification

Fangfang Ma,[ab] Gaoshun Ge,[ab] Yizhen Fang,[ab] Erru Ni,[ab] Yuanyuan Su,[ab] Fan Cai *[c] and Huabin Xie *[ab]

Rapid and accurate identification of cardiac troponin I (cTnI) in biological fluids is very essential for judging acute myocardial infarction (AMI). Herein, we constructed an enzyme-free electrochemical immunosensing system for sensitive monitoring of human plasma cTnI cardio-cerebrovascular diseases. Prussian blue-doped PAMAM dendrimer nanospheres (PBDENPs) were first synthesized by using *in situ* chemical reaction, and functionalized with polyclonal anti-human cTnI antibody as the signal-transduction tags. Field-emission transmission electron microscopy (FETEM), dynamic light scattering (DLS), and scanning electron microscopy (SEM) were utilized for characterization of the immunosensing platform. By using a monoclonal anti-human cTnI antibody-modified screen-printed carbon electrode (SPCE) as the immunsensing interface and polyclonal anti-cTnI antibody-labeled PBDENPs and the signal tags, a new sandwich-type immunoassay was designed for the determination of target cTnI by using square wave voltammetry (SWV). Multi-armed dendritic PAMAM nanospheres were expected to enhance the detectable signal of electrochemical immunoassay through the doped Prussian blue with electrochemical activity. Under optimum conditions, the enzyme-free electrochemical immunoassay displayed a wide linear range of four orders of magnitude from 0.01 ng mL^{-1} to 100 ng mL^{-1} with a low detection limit of 6.2 pg mL^{-1} cTnI at the $3s_B$ criterion. An intermediate precision of $\leq$10.9% was accomplished with batch-to-batch identification, and good anti-interference capacity against other cancer biomarkers or proteins was acquired toward target cTnI. In addition, measurements of human serum specimens were demonstrated to further confirm the method accuracy of electrochemical immunoassay, and well-matched results were obtained between the electrochemical immunoassay and the referenced enzyme-linked immunosorbent assay (ELISA) method.

Received 27th March 2021,
Accepted 23rd April 2021

DOI: 10.1039/d1nj01506k

rsc.li/njc

Introduction

Acute myocardial infarction (AMI), a severe and lethal coronary heart disease, is a major cause of ischemic cardiomyopathy with extremely high disability and mortality.[1] AMI occurrence mainly results from the long-time ischemia of myocardial cells to trigger morphological changes of the myocardium and myocardial fibroblasts due to oxidative stress, leading to myocardial cell death.[2] Cardiac-specific troponins, such as cardiac troponin T (cTnT) and cardiac troponin I (cTnI), are important circulating biomarkers of myocardial cell damage, and are used for the investigation of suspected myocardial ischaemia in modern clinical practice.[3] Therefore, evaluation of cTnT/or cTnI is an essential criterion for the diagnosis of AMI. Cardiac troponin I with a molecular weight of 37 kDa acts as a molecular switch for the activation of the cardiac thin filament by coupling Ca(II) binding to troponin C.[4] The cTnI is an ideal biomarker for myocardial injury.[5] The concentration of cTnI in a healthy person is below $\sim$0.5 ng mL^{-1}, and increases within 4-6 h after onset of chest pain. As is well known, cTnI is an important prognostic indicator for heart disease and the suggested clinical cutoff value of cTnI is 0.06–1.5 ng mL^{-1}.[6] In this case, diagnosis at the early stage of cTnI is crucial for effective treatment of AMI patients.

Recently, different methods and strategies have been reported for the detection of target cTnI using immunoassays and aptasensors.[7,8] Electrochemical immunoassays, based on

[a] *Clinical Laboratory Department, Xiamen Cardiovascular Hospital of Xiamen University, Xiamen City, Fujian Province, China. E-mail: huabinxie@yeah.net*
[b] *Xiamen Key Laboratory of Precision Medicine for Cardiovascular Disease, Xiamen City, Fujian Province, China*
[c] *College of Life Sciences, Fujian Normal University, Fuzhou 350117, China. E-mail: caif@fjnu.edu.cn*

specific antigen–antibody reaction, have gained increasing attention for quantitative screening of disease-related proteins because of simple instrumentation and easy signal quantification.[9–11] For developing a good electrochemical immunosensing platform, one key point is how to generate a strong electrochemical signal after the antigen–antibody reaction. Typically, enzymes (*e.g.*, horseradish peroxidase and alkaline phosphatase) and electroactive indicators (*e.g.*, ferricyanide, ferrocene, methylene blue, thionine and Prussian blue) are usually employed to produce electrochemical signals.[12–14] Despite the high sensitivity of enzyme-based immunoassays, they have some disadvantages: (i) detectable signals are susceptible to interference during the assay because the signal generation must be controlled and optimized, in much the same way as antigen–antibody reaction; and (ii) enzyme-substrate incubation is sensitive to time, temperature and pH, and inhibitory substrates should be absent.[15] An alternative sensing strategy that is based on an electrochemical principle and does not require an enzyme reaction would be advantageous. Inspiringly, the emergence of electroactive indicators open a new horizon for development of electrochemical immunoassays.[16,17] Prussian blue, $Fe_4[Fe(CN)_6]_3$, exhibits great potential because it can be easily excited to induce its catalytic function due to its low energy gap.[18,19] Thanks to various valances of iron in its unit cell, Prussian blue can produce electron movement for easy oxidation or reduction *via* external potential.[20] In this regard, Prussian blue can be utilized as an indicator for the readout of electrochemical signal during the immunoassays.

Another important issue is how to fabricate Prussian blue-based electrochemical immunoassay with signal amplification. An advisable method is to exploit high-efficient signal-transduction labels (tags) by using Prussian blue nanoparticles. Luo *et al.* used gold nanoparticles functionalized hollow mesoporous Prussian blue nanoparticles as the electrochemical probes for detecting protein biomarker.[21] Tang *et al.* used core–shell magnetic bead-Prussian blue nanocomposites as the labels for electrochemical immunoassay of human IgG.[22] It is well-known that the loading amount of Prussian blue in the mesoporous or core–shell nanostructures is limited. Dendrimers, repetitively branched molecules with the spheroidal structures, are precisely supervised to load specific ions entrapped into the interior void spaces or attached on the surface.[23,24] To this end, dendrimers are usually utilized to synthesize monodisperse nanospheres because one dendrimer has hundreds of sites for conjugation with an active species. Typically, Prussian blue nanoparticles are synthesized on the basis of chemical reaction between $[Fe(CN)_6]^{4-}$ and Fe^{3+} ions under certain conditions.[18] Based on this consideration, our motivation of this study is to synthesize Prussian blue-doped poly(amidoamine) (PAMAM) dendrimer inorganic–organic nanospheres for the labelling of biomolecules in the immunosensing system.

By using cardiac troponin I (cTnI) as the target analyte, we design an electrochemical immunoassay for the voltammetric detection of cTnl (Scheme 1). The sandwich-type immunoreaction is carried out on the capture antibody-modified screen-printed carbon electrode (SPCE) using Prussian blue-doped PAMAM dendrimer nanoparticles as the signal-transduction tags. The voltammetric signal derives from the doped Prussian blue in the nanospheres within the applied potentials. The use of PAMAM dendrimer is expected to enhance the sensitivity of the electrochemical immunoassay. The major objective of this work is to explore a new enzyme-free electrochemical immunoassay for sensitive detection of low-abundance proteins by using Prussian blue aggregated dendrimer microspheres.

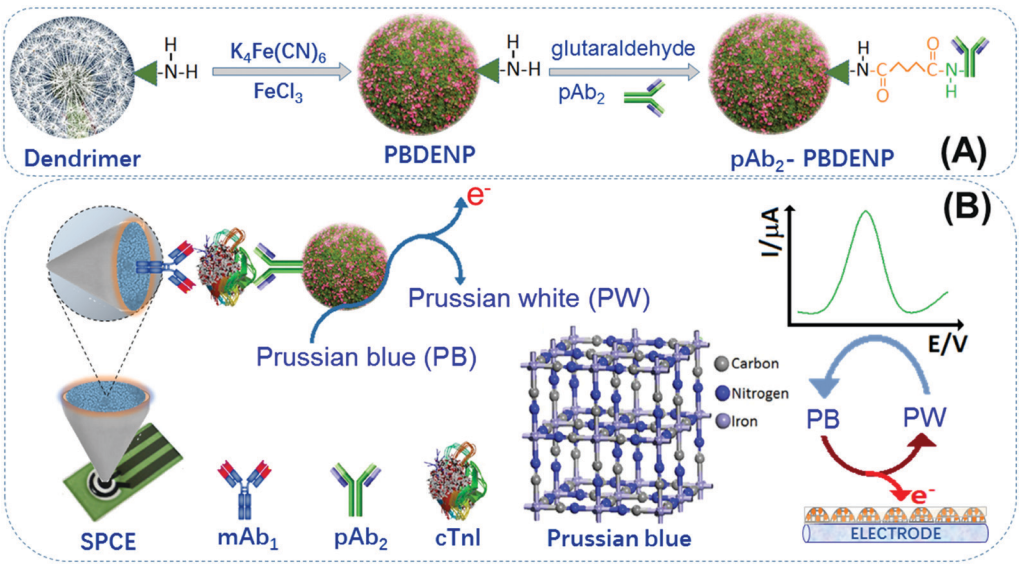

Scheme 1 Schematic illustration of enzyme-free electrochemical immunoassay for human plasma cardiac troponin I (cTnl) with enzymatic amplification by using Prussian blue-doped PAMAM dendrimer nanosphere (PBDENP) as the signal-transduction tag: (A) preparation process of polyclonal rabbit anti-human cardiac troponin I antibody (pAb_2)-labeled PBDENP (pAb_2-PBDENP), and (B) immunoreaction protocol and electrochemical measurements toward target cTnl on monoclonal rabbit anti-human cardiac troponin I antibody (mAb_1)-coated screen-printed carbon electrode (SPCE) with a sandwich-type assay format by using square wave voltammetry.

Experimental section

Material and chemical

Monoclonal rabbit anti-human cardiac troponin I antibody (mAb_1; EPR20307, cat#: ab209809) and polyclonal rabbit anti-human cardiac troponin I antibody (pAb_2; cat#: ab155047) were purchased from Abcam (Shanghai, China). Human cardiac troponin I (cTnI) ELISA kits were obtained from ThermoFisher Sci. (Shanghai, China) (sensitivity: 100 pg mL^{-1}; 125–8000 pg mL^{-1}; cat#: EHTNNI3). All screen-printed carbon electrodes were purchased from Metrohm AutoLab Inc. (Netherlands), which contained a carbon working electrode (active area: 4.125 mm^2), carbon counter electrode and Ag/AgCl reference electrode. The PAMAM dendrimer (ethylenediamine core, generation 5.0 solution, 5.0 wt% in methanol), bovine serum albumin (BSA; Vetec™, reagent grade, lyophilized powder, ≥98%), glutaraldehyde solution (50 wt% in H_2O), and other chemicals were acquired from Sigma-Aldrich (Merck KGaA, Darmstadt, Germany). Ultrapure water from a Milli-Q water purification system (18.2 MΩ cm, Millipore) was used throughout this work. All buffers including phosphate-buffered saline (PBS) solution were the product of Sigma.

Synthesis of Prussian blue-doped PAMAM dendrimer nanospheres

Prussian blue-doped PAMAM dendrimer nanospheres (PBDENPs) were synthesized through an *in situ* chemical reaction method similar to this literature.[25] Initially, the PAMAM dendrimer in methanol (1.0 mL, 5.0 wt%) was added into 8.0-mL methanol, and then 1.0 mL of $K_4Fe(CN)_6$ methanolic solution (2.0 M) was injected into the mixture. Following that, the resulting mixture was generally shaken on a shaker for 6 h at room temperature. During this process, the negatively charged $[Fe(CN)_6]^{4-}$ ions were penetrated into the interior void spaces of the dendrimers, and adsorbed on the surface of positively charged amino groups. Afterwards, 1.0 mL of $FeCl_3$ (2.0 M) in methanol was thrown into the mixture to form Prussian blue nanostructures under the same conditions. To remove free Prussian blue nanoparticles outside of the dendrimers, the resultant suspension was centrifuged for 10 min at 8000*g* at room temperature. The obtained precipitation was collected and washed with methanol/water several times. Finally, the as-prepared PBDENPs were dried in a vacuum and stored at 4 °C for use. As control tests, Prussian blue nanoparticles alone without the PAMAM dendrimer were synthesized using a similar method.

Conjugation of PBDENP with pAb_2 antibody (pAb_2-PBDENP)

Polyclonal anti-cTnI pAb_2 antibody was labeled onto the surface of PBDENP nanohybrids through typical glutaraldehyde referring to the literature.[26] In detail, the above-synthesized PBDENPs (20 mg) were first dispersed into PBS (2.0 mL, 10 mM, pH 7.4) containing 500 μL, 50 wt% glutaraldehyde (note: excess glutaraldehyde should be used at this step to avoid possible conjugation between PBDENPs). Then, the resulting suspension was incubated for 6 h at room temperature under gentle stirring to make the PBDENPs functionalized with aldehyde group. Following that, the mixture was centrifuged for 10 min at 8,000*g*, and the obtained pellets was redispersed in PBS (2.0 mL, 10 mM, pH 7.4). 200 μL of carbonate buffer (pH 9.6) containing pAb_2 (100 μg mL^{-1}) was added into the mixture, and incubated for 12 h at 4 °C under gentle shaking on a shaker. The resulting suspension was centrifuged as before, and the obtained pellets were thrown into sodium cyanoborohydride (1.0 mL, 5.0 mg mL^{-1}). The mixture was reacted for 60 min at room temperature to reduce the resulting Schiff bases and any excess aldehyde. Finally, the collected pAb_2-PBDENP conjugates by centrifugation was dispersed in PBS (1.0 mL, 10 mM, pH 7.4), and stored at 4 °C when not in use ($C_{[pAb2\text{-}PBDENP]} \approx 20$ mg mL^{-1}).

Preparation of electrochemical immunosensor

All the electrochemical immunosensors were prepared by modifying mAb_1 antibodies onto the screen-printed carbon electrodes (SPCEs) with BSA colloids. Initially, the purchased SPCE was rinsed completely with successive sonication in ultrapure water and absolute ethanol, alternately. The SPCE was then dried by a hair dryer for later use. Prior to modification, colloidal BSA containing the antibody was prepared by mixing mAb_1 (100 μL, 50 μg mL^{-1}) with BSA aqueous solution (400 μL, 20 wt%). The resulting mixture was adequately shaken to make mAb_1 antibodies disperse homogeneously in the suspension. After that, 100 μL of the above-prepared mAb_1-BSA colloids was dropped onto the working electrode of SPCE, and dried in the oven at 37 °C. Finally, the resultant electrode was slightly washed with PBS (10 mM, pH 7.4), and stored at 4 °C for subsequent usage.

Immunoreaction process and voltammetric measurement

Scheme 1 gives the schematic illustration of electrochemical sensing platform for voltammetric detection of target cTnI on mAb_1-coated SPCE with a sandwiched immunoreaction mode using pAb_2-PBDENP as the secondary antibody. The immunoreaction was carried out as follows: (i) 100 μL of different-concentration cTnI sample was thrown onto the mAb_1-coated SPCE, and incubated for 40 min at 37 °C for the capture of target cTnI; and (ii) after being washed with PBS (10 mM, pH 7.4), 100 μL of pAb_2-PBDENP suspension (20 mg mL^{-1}) was dropped onto the resultant SPCE, and incubated for 40 min under the same conditions to form the sandwiched immunocomplex. Following that, the voltammetric current of the resulting SPCE was monitored in PBS (10 mM, pH 5.5) using square wave voltammetry (SWV) from 50 mV to 450 mV (*vs.* Ag/AgCl) (amplitude: 25 mV; frequency: 15 Hz; increase *E*: 4.0 mV). The obtained voltammetric peak current (μA) was collected and registered as the signal of the immunosensor for different concentrations of the target cTnI. The sigmoidal curve was obtained by mathematically fitting experimental points by using the Rodbard's four-parameter function with the Origin 8.0 software. Graphs were plotted in the form of voltammetric current against the logarithm of cTnI concentration. All measurements were carried out in triplicate at room temperature

(25 ± 1.0 °C). The results are expressed as mean value ± standard deviation (SD) of 3 determinations and statistical significance was defined at $P \leq 0.05$.

Measurement of human serum samples with cTnI ELISA kit

For reference, a commercial human cTnI ELISA assay was employed to determine human serum specimens for method comparison study. Before measurements, all human serum samples were centrifuged for 10 min at 5000*g* to remove possible precipitates. Afterword, these serum specimens were determined using commercialized cTnI ELISA kit. 50 μL of the serum sample was added into the standard polystyrene plate, and incubated for 60 min at 37 °C. The plate was rinsed three times (3 min each) with PBS (0.1 M, pH 7.4) containing 0.5 M NaCl and 1.0 M Tween 20. Thereafter, 50 μL of enzyme-based conjugates was added into the well, and reacted for 60 min at 37 °C. The plate was washed again, and 3,3′,5,5′-tetramethylbenzidine (TMB; 50 μL) was added and incubated for 10 min at 37 °C. Finally, enzymatic reaction was stopped by H_2SO_4 (50 μL per well, 2.0 M), and the result of the ELISA was measured on a spectrophotometric ELISA reader at a wavelength of 450 nm.

Results and discussion

Design motivation of electrochemical immunoassay with PBDENP

Methods based on electrochemical measurement have been largely reported for immunoassay development, but most involve enzyme labels or nano labels. For the development of advanced electrochemical immunoassays, signal amplification and noise reduction are crucial during the signal-generation stage. Generally, enzyme-labeled assays are usually carried out in the solution containing redox couples, thus resulting in high background signal. In this work, the immunosensor is prepared using BSA without redox reaction, whereas an electroactive Prussian blue indicator is labeled onto the secondary antibody for the signal generation. In this case, voltammetric signal can be acquired after the antigen–antibody reaction. The mAb_1-coated SPCE with the BSA exhibits a relatively low background signal with noise reduction. Introduction of a Prussian blue-doped PAMAM dendrimer is expected to amplify the detectable signal of electrochemical immunosensor. Prussian blue nanoparticles with electrochemical activity are doped into the PAMAM dendrimer through *in situ* chemical reaction. Anti-cTnI pAb_2 antibody is conjugated onto the PAMAM dendrimer *via* the cross-linkage glutaraldehyde reagent. In the presence of target cTnI, the electroactive pAb_2-PBDENP with redox properties is attached on the surface of electrode, thereby causing strong voltammetric signal within the applied potentials. The corresponding peak current relies on the concentration of the target cTnI in the sample according to the rule of sandwiched immunoreaction. With the increment of target cTnI concentration, the conjugated amount of pAb_2-PBDENPs on the electrode increased, thus quantitatively monitoring the level of cTnI.

Characterization of pAb_2-PBDENP and mAb_1-SPCE

In this work, the electrochemical immunoassay involves mAb_1-SPCE and pAb_2-PBDENPs. Addition of target cTnI can cause the formation of immunocomplex between mAb_1-SPCE and pAb_2-PBDENPs. In this case, we first used different methods to characterize the prepared mAb_1-SPCE and pAb_2-PBDENPs. Fig. 1A shows field emission transmission electron microscopy images (FETEM; FEI Talos F200S G2, Thermo Scientific, USA) of Prussian blue-doped PAMAM dendrimer nanospheres. Most of the PBDENPs were homogeneously dispersed into the solution, and the average size was ~60 nm in diameter. As expected, elemental mapping images demonstrated the homogeneous distributions of iron, carbon, nitrogen and oxygen over the entire architecture of PBDENP nanospheres (Fig. 1B–E). Moreover, the content of iron (Fe) element in PBDENPs was quantified to be 1.83 wt% by inductively couple plasma optical emission spectrometry (ICP-OES).

To further characterize the as-synthesized PBDENPs, we also used dynamic light scattering (DLS; Zetasizer Nano S90, Malvern, London, UK) to monitor the sizes of the PBDENPs before and after conjugation with pAb_2. As shown in Fig. 1F, the mean size of pAb_2-PBDENPs (76 ± 3.1 nm, upper) was more than that of the as-prepared PBDENPs (68 ± 2.3 nm, bottom). The increasing size should derived from the labeled biomolecules including the glutaraldehyde and antibody. The size of PBDENPs obtained by DLS was bigger than that obtained by FETEM, which was ascribed to the fact that the size of DLS originated from hydration radius of nanoparticles. Logically, a puzzling question arises as to whether anti-cTnI pAb_2 antibodies were really conjugated onto the PBDENPs. To clarify this

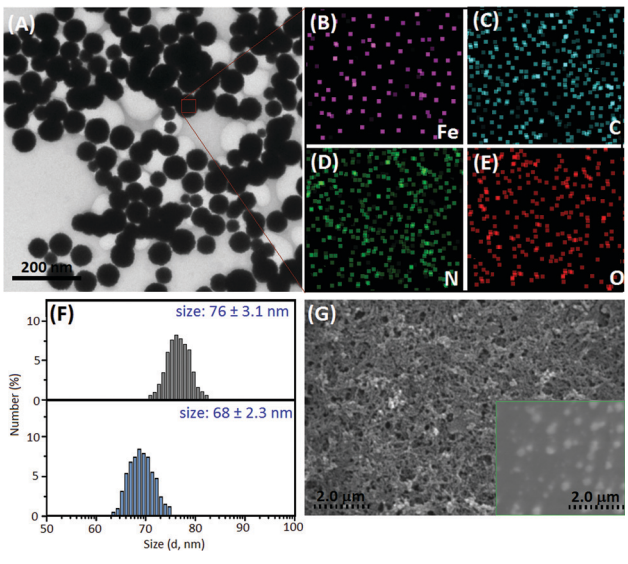

Fig. 1 (A) HAADF-STEM image of PBDENP; (B–E) element mapping for Fe, C, N and O of PBDENP; (F) DLS data of (bottom) PBDENP and (upper) pAb_2-PBDENP; (G) SEM image of mAb_1-BSA-SPCE (inset: SEM image of cleaned SPCE.

issue, the zeta potentials of pAb_2-PBDENPs after each step were studied with the DLS. A negative zeta potential (ζ = −10.6 mV) was observed at the as-prepared PBDENPs, which stemmed from the negatively charged hydroxyl groups on the Prussian blue nanostructures. After reaction with the glutaraldehyde, the zeta potential of PBDENPs decreased to −3.8 mV, and the reason was most likely a consequence of the fact that negatively charged hydroxyl groups were replaced by the aldehyde group with no charge. Significantly, the zeta potential increased to −19.3 mV after aldehydic PBDENPs reacted with pAb_2 antibodies. Typically, antibody is a kind of protein with an isoelectric point. Since the isoelectric point of anti-cTnI antibody is less than pH 7.4, it is a negatively charged species in pH 7.4 PBS. The results revealed the successful preparation of pAb_2-PBDENP.

Next, the fabrication process of immunosensor was characterized by using scanning electron microscopy (SEM; Hitachi 4800, Japan). The inset of Fig. 1G represents a typical SEM image of cleaned SPCE, and the surface was relatively smooth. When mAb_1-BSA colloids were coated on the surface of SPCE, however, the surface became rougher (Fig. 1G). There seem to be numerous materials covering the surface of the electrode, indicating that mAb_1-BSA-modified membrane could be formed on the cleaned SPCE.

Electrochemical characteristics of immunosensor

Electrochemical impedance spectroscopy (EIS) gives information on the impedimetric changes of immunosensor during the modification process.[27,28] Fig. 2A shows typical Nyquist diagrams of variously modified electrodes after each step in PBS (10 mM, pH 7.4) containing 10 mM $[Fe(CN)_6]^{4-/3-}$ solution, and the inset of Fig. 2A represents the fitting Randles equivalent circuit on the basis of EIS data, which consisted of electrolyte resistance (R_s), lipid bilayer capacitance (C_{dl}), charge transfer resistance (R_{ct}) and Warburg element (Z_w). The complex impedance can be presented as the sum of the real, Z_{re} and imaginary, Z_{im}, components that originate from the resistance and capacitance of the cell. The two components of the scheme, R_s and Z_w, represent the bulk properties of electrolyte solution and diffusion of applied redox probe in solution, respectively. Thus, they are not affected by chemical transformations occurring at the electrode interface. The other two components of circuit, C_{dl} and R_{ct}, depend on the dielectric and insulating features at the electrode/electrolyte interface. In EIS, the semicircle diameter of EIS equals the electron transfer resistance, R_{ct}. This resistance controls electron transfer kinetics of the redox-probe at the electrode interface, and the value varies when different substances are adsorbed onto the electrode surface. Nyquist '*a*' gives the EIS of cleaned SPCE with a small resistance of ~512 Ω. In contrast, the resistances increased when bare SPCE was modified with mAb_1-BSA (Nyquist '*b*'), indicating that biomacromolecules hindered electron transfer of ferricyanide from solution to the base electrode. Following that, the as-prepared immunosensor was utilized to detect target cTnI (0.1 ng mL^{-1} used as an example). Obviously, introduction of target cTnI (Nyquist '*c*') and pAb_2-PBDENP (Nyquist '*d*') caused the increasing resistances of the modified electrodes in sequence.

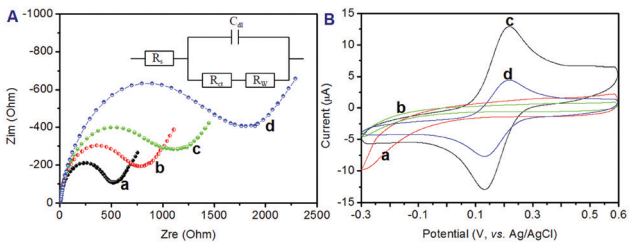

Fig. 2 (A) Nyquist diagrams for (a) SPCE, (B) mAb_1-BSA-SPCE, (c) cTnI/mAb_1-BSA-SPCE and (d) pAb_2-PBDENP/cTnI/mAb_1-BSA-SPCE in PBS (10 mM, pH 7.4) containing 10 mM $Fe(CN)_6^{4-/3-}$ and 0.1 M KCl within the range from 10^{-2} Hz to 10^5 Hz at an alternate voltage of 5.0 mV (inset: equivalent circuit); (B) cyclic voltammograms for (a) mAb_1-BSA-SPCE, (b) cTnI/mAb_1-BSA-SPCE, (c) pAb_2-PBDENP/cTnI/mAb_1-BSA-SPCE and pAb_2-PBNP/cTnI/mAb_1-BSA-SPCE in PBS (10 mM, pH 5.5) at 50 mV s^{-1} (note: 0.1 ng mL^{-1} cTnI used in these cases).

As mentioned above, the main purpose of this work is to fabricate a voltammetric immunoassay for screening disease-related protein. To investigate the feasibility of the immunosensor, differently modified electrodes were monitored in PBS (pH 5.5, 10 mM) by using cyclic voltammetry at 50 mV s^{-1} (Fig. 2B). No cyclic voltammetric peak was observed at both mAb_1-BSA-SPCE (curve '*a*') and cTnI/mAb_1-BSA-SPCE (curve '*b*') within the working potential range. However, the background current decreased after the as-prepared mAb_1-BSA-SPCE reacted with target cTnI (0.1 ng mL^{-1}), indicating that the formed immunocomplexes was unfavourable for the electron transfer. In contrast, stable and well-defined redox peaks at +140 mV and +230 mV were acquired when the resulting immunosensor was incubated again with pAb_2-PBDENP conjugates in PBS (pH 5.5, 10 mM) (curve '*c*'). The redox peaks derived from the doped Prussian blue. Therefore, the as-prepared PBDENP could be used as an indicator for the detection of target cTnI. Maybe, one question to be produced is whether the electroactive pAb_2-PBDENP could amplify the detectable signal of the electrochemical immunosensor for the detection of target cTnI. To further demonstrate the amplified efficiency of electrochemical immunosensor using pAb_2-PBDENP, a comparative study was carried out with and without the PAMAM dendrimer (*i.e.*, by using Prussian blue nanoparticle-labeled pAb_2 antibody; pAb_2-PBNP). Note that Prussian blue nanoparticle-labeled pAb_2 antibodies were prepared by using (3-glycidyloxypropyl)trimethoxysilane similar to the literature studies.[29,30] The evaluation was carried out on the basis of peak current change (*versus* background signal) toward the same-concentration cTnI. As indicated from Fig. 2B, the immunosensor by using pAb_2-PBNP gave a relatively small current variation (Δi = 3.28 μA, curve '*d*' *vs.* curve '*a*'). In contrast, a big current variation was acquired by using pAb_2-PBDENP (Δi = 7.39 μA, curve '*c*' *vs.* curve '*a*'). The use of pAb_2-PBDENP could cause a 225.3 ± 8.6% current increase of the immunosensor toward 0.1 ng mL^{-1} cTnI. The reason was ascribed to the fact that PAMAM dendrimer could

simultaneously accommodate more PBNPs into the cavity. When one antibody on pAb_2-PBDENP reacted with the target cTnI, all the loaded PBNPs in the dendrimer could enforce the voltammetric signal, thereby resulting in the signal amplification.

Optimization of experimental conditions

In this system, the assay involves the antigen–antibody reaction and voltammetric measurements. Generally, the immunoreaction is readily implemented at human normal temperature (~37 °C) for the antigen–antibody conjugation. However, it usually takes some time for the antigen–antibody reaction. Under these conditions, we investigated the effect of immunoreaction time on the SWV peak current of the electrochemical immunoassay (note: The incubation time between cTnI and mAb_1 was paralleled with pAb_2-PBDENP and target analyte). As shown in Fig. 3A, the voltammetric peak current initially increased with the increasing immunoreaction time, and then tended to level off after 40 min. To achieve an adequate reaction between antigen and antibody, and also save the assay time, an incubation time of 40 min was chosen for the antigen–antibody reaction.

The effect of pH on the voltammetric signal of the immunosensor was studied between 3.0 and 8.0 for PBS detection solution (10 mM). As seen from Fig. 3B, the voltammetric peak currents increased from 3.0 to 5.5, and decreased from 5.5 to 8. Generally, the electron mediators including Prussian blue have good redox efficiency under the optimum pH conditions. Obviously, improved voltammetric peak current was obtained at pH 5.5 PBS (10 mM). Therefore, PBS of pH 5.5 (10 mM) was used as the supporting electrolyte for voltammetric measurement of the electrochemical immunosensor.

Voltammetric responses of immunosensor toward cTnI standards

By using square wave voltammetry, the as-prepared mAb_1-BSA-SPCE was utilized for voltammetric detection of target cTnI standards with different concentrations under optimum conditions. The assay was carried out in a sandwich-type immunoreaction mode using pAb_2-PBDENP as the signal-transduction tag. Fig. 4A shows the SWV curves of the immunosensor toward cTnI standards with various levels in 10 mM PBS (pH 5.5). It can be seen that the change of peak currents at +230 mV was small at the lower or higher cTnI concentration range, and exhibited a sigmoidal relationship between peak currents and the logarithm of cTnI concentrations (Fig. 4B). Inspiringly, a good linear relationship could be found from 0.01 to 100 ng mL^{-1} cTnI. The detection limit could be estimated to 6.2 pg mL^{-1} at the $3S_{blank}$ level (n = 11). The linear regression equation was y = 12.16 + 5.48 × log $C_{[cTnI]}$ (ng mL^{-1}, n = 15) with a correlation coefficient of 0.9871. According to the linear regression equation, we could quantitatively calculate the target cTnI level in the sample. Moreover, the analytical properties of our system were comparable with those of other cTnI detection methods including the linear range and LOD (Table 1). Furthermore, our strategy also exhibited a lower LOD in comparison with commercial cTnI ELISA kits (*e.g.*, 100 pg mL^{-1} for Sigma-Aldrich RAB0634, 2.0 ng mL^{-1} for Biolead 600-410-CTN, 100 pg mL^{-1} for ThermoFisher EHTNNI3, 78 ng mL^{-1} for Nova Lifetich Inc ELA-E0478h), and 11.75 pg mL^{-1} for CUSABIO® CSB-305139h).

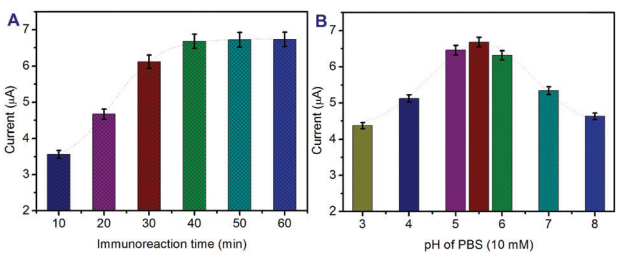

Fig. 3 Dependence of the SWV peak current of pAb_2-PBDENP-based electrochemical immunosensor on (A) immunoreaction time for the antigen–antibody conjugation and (B) PBS-based detection solution (10 mM) by using 0.1 ng mL^{-1} cTnI as an example.

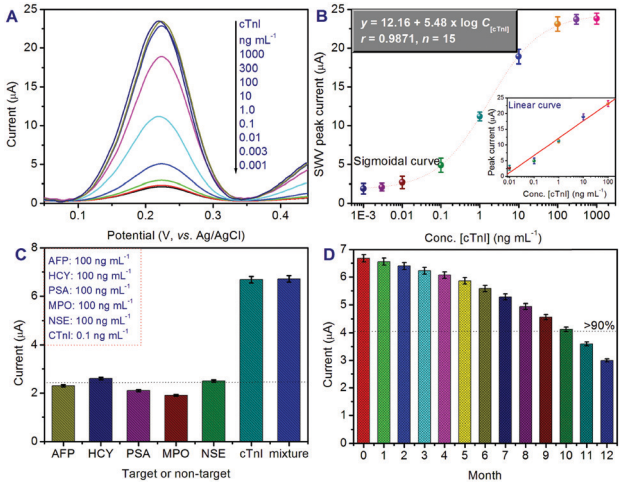

Fig. 4 (A) SWV data plots of the pAb_2-PBDENP-based electrochemical immunosensor toward cTnI standards with different concentrations in PBS (10 mM, pH 5.5); (B) calibration curve for the relationship between peak current and decimal logarithm of cTnI concentration; (C) specificity of electrochemical immunosensor against target cTnI, AFP, HCY, PSA, MPO and NSE (note: the mixture contained the above-mentioned analytes); (D) the storage stability of mAb_1-BSA-SPCE and pAb_2-PBDENP at 4 °C for intermittent measurements (every month) of 0.1 ng mL^{-1} cTnI.

Reproducibility, specificity and stability of immunosensor

The precision of the PBDENP-based electrochemical immunosensor was evaluated by calculating intra- and inter-batch variation coefficients (CVs, n = 5) toward 3 cTnI standards with different concentrations. Table 2 displays the experimental results for various cTnI samples. The CVs were less than 7.60% for intra-assay and 10.9% for inter-assay in these cases. Hence, the repeatability and intermediate precision of electrochemical immunosensor was acceptable.

To evaluate the specificity of the electrochemical immunosensor, the as-prepared mAb_1-BSA-SPCE and pAb_2-PBDENP were used for other proteins or biomarkers, *e.g.*, alpha-fetoprotein (AFP), homocysteine (HCY), prostate-specific

Table 1 Comparison of analytical properties between the PBDENP-based electrochemical immunosensor and other electrochemical sensing systems for target cTnl

Method	Linear range (ng mL^{-1})	LOD (pg mL^{-1})	Ref.
Electrochemiluminescent immunosensor	0.005–200	3.2	31
Electrochemiluminescentimmunosensor	0.0001–50	0.03	32
Voltammetric immunosensor	0.001–100	0.39	33
Electrochemical aptasensor	0.01–100	7.5	34
Electrochemical aptasensor	0.05–100	16	35
Potentiometric immunosensor	0.01–10	7.3	36
Amperometric immunosensor	0.05–3.0	50	37
Impedimetric immunosensor	0.2–10	200	38
Voltammetric immunosensor	0.01–100	6.2	This work

Table 2 Intra- and inter-batch variation coefficients (CVs) for intra-assay and inter-assay of electrochemical immunosensor

		Time; conc. (ng mL^{-1})					
Type	Conc. ng mL^{-1}	1	2	3	4	5	CV (%)
Intra-assay	0.05	0.056	0.047	0.048	0.053	0.053	7.36
	1.0	0.89	1.08	1.03	0.94	0.97	7.60
	50	52.3	51.4	47.4	53.8	49.3	4.96
Inter-assay	0.05	0.059	0.052	0.046	0.048	0.043	10.9
	1.0	0.87	1.12	1.11	1.08	1.07	9.78
	50	54.6	47.1	51.4	47.2	54.8	7.23

antigen (PSA), myeloperoxidase (MPO), and neuron-specific enolase (NSE). Experimental results for voltammetric immunosensor obtained for each non-target analyte presented at a concentration of 100 ng mL^{-1} was compared with that of 0.1 ng mL^{-1} cTnl, and the ratio (1000 : 1) was used as a criterion for the specificity of immunosensor. The evaluation was executed as follows: (i) all the analytes including cTnl, AFP, HCY, PSA, MPO and NSE with the above-mentioned levels were individually measured with this sensor, and (ii) the mixture containing target cTnl and non-targets (*i.e.*, AFP, HCY, PSA, MPO and NSE) with the above concentrations were determined using this immunosensor. As shown in Fig. 4C, high SWV peak currents were acquired in the presence of target cTnl, and other non-targets almost did not interfere with the SWV responses of the immunosensor. So, the electrochemical immunosensor had good specificity toward cTnl.

Table 3 Analysis of 8 clinical specimens of human serum containing target cTnl (collected from the patients with cardio-cerebrovascular diseases) using the electrochemical immunosensor and human cTnl ELISA kit

	Method; conc. (mean ± SD, ng mL^{-1}; n = 3)[a]		
No.	Immunosensor	ELISA kit	RSD (%)
1	145.1 ± 3.7	141.9 ± 2.4	1.58
2	89.2 ± 2.3	92.1 ± 2.7	2.26
3	23.4 ± 1.7	22.4 ± 1.8	3.09
4	6.5 ± 0.53	6.2 ± 0.42	3.34
5	13.9 ± 0.12	14.8 ± 0.17	4.43
6	36.3 ± 1.4	39.6 ± 1.2	6.15
7	73.1 ± 2.1	71.6 ± 2.6	1.47
8	69.2 ± 2.8	70.3 ± 2.3	1.12

[a] High concentrations were calculated referring to the dilution ratio.

The long-term storage stability of electrochemical immunosensor was studied for a 12-month period. When the prepared mAb_1-BSA-SPCE and pAb_2-PBDENP were stored at 4 °C and measured (every one month), no apparent change for the same cTnl concentration was found over 10 months (Fig. 4D). Good long-term stability might be attributed to the covalent conjugation of pAb_2 with the PBDENP and the encapsulation efficiency of BSA colloids for mAb_1.

Application of the immunosensor in human serum samples

The analytical reliability and applicable potential of the electrochemical immunosensor were evaluated by analysing 8 clinical specimens of human serum containing target cTnl. These samples were collected from the patients with cardio-cerebrovascular diseases at laboratory department of our hospital according to the ethical standards of the local hospital. These samples were first centrifuged (10 min, 5000*g*) to remove the possible precipitates, and then detected by using the developed immunosensor (note: high-concentration samples were diluted within the linear range of the immunosensors by 10 mM pH 7.4 PBS). As the reference, these specimens were also measured by using commercial human cTnl ELISA kit. Table 3 listed experimental results for these samples. The relative standard deviations (RSDs) for these sample between two methods were less than 7.0%, indicating a good accuracy of the electrochemical immunosensor for the analysis of target cTnl toward complex human serum samples.

Conclusions

This contribution fabricated a new electrochemical immunosensing platform for voltammetric determination of target cTnl in biological fluids from the patients with cardio-cerebrovascular disease. Results indicated that the development electrochemical immunoassay had high sensitivity, good reproducibility and specificity, and acceptable method accuracy for the target cTnl analyte. Relative to previous reports on electrochemical immunosensors/or immunoassays, our designed system has the following advantages: (i) the immunosensing system does not involve the participation of natural enzymes, thus efficiently avoiding the interference from enzyme substrates; (ii) Prussian blue-doped PAMAM dendrimer nanospheres are used as electroactive indicators, thereby avoiding the participation of electron mediators

during the voltammetric measurement; and (iii) capture antibodies are directly modified onto the electrode with the protein membrane for the decreasing background currents. In addition, the PBDENP-based electrochemical immunosensor is capable of continuously carrying out all steps less than 100 minutes for one sample including incubation, washing, and electrochemical measurement.

Compliance with ethical standards

All the experiments were performed in compliance with the relevant laws and Guidelines of Xiamen Cardiovascular Hospital of Xiamen University (China) and the experiments have been approved.

Informed consent was obtained for any experimentation with human subjects.

Conflicts of interest

There are no conflicts to declare.

Acknowledgements

This work was supported by the Medical and Health Guidance Project of Xiamen (grants: 3502Z20209140 & 3502Z20209139), and the Medical Innovation Project of Fujian Provincial Health Commission (grant: 2019-CXB-37).

References

1 J. Reyes-Retana and L. Duque-Ossa, *Curr. Problems Cardiol.*, 2021, **46**, 100739.
2 G. Kassimis and F. Picard, *Cardiology*, 2019, **142**, 97–99.
3 Y. Saito and Y. Kobayashi, *J. Cardiol.*, 2019, **74**, 95–101.
4 T. Lalem and Y. Devaux, *Clin. Chem.*, 2019, **70**, 1–7.
5 K. Dhara and D. Mahapatra, *Microchem. J.*, 2020, **156**, 104857.
6 M. Zaninotto, A. Padoan, M. Mion, M. Marinova and M. Plebani, *Clin. Chim. Acta*, 2020, **504**, 163–167.
7 P. Kavsak, V. Tandon and C. Ainsworth, *Clin. Chem.*, 2020, **66**, 854–855.
8 X. Mi, H. Li, R. Tan and Y. Tu, *Anal. Chem.*, 2020, **92**, 14640–14647.
9 J. Shu and D. Tang, *Anal. Chem.*, 2020, **92**, 363–377.
10 J. Shu and D. Tang, *Chem. – Aisan J.*, 2017, **12**, 2780–2789.
11 S. Ge, Y. Zhang, M. Yan, J. Huang and J. Yu, *Methods Mol. Biol.*, 2017, **1527**, 125–134.
12 Z. Yu, G. Cai, X. Liu and D. Tang, *Anal. Chem.*, 2021, **93**, 2916–2925.
13 Z. Luo, Q. Qi, L. Zhang, R. Zeng, L. Su and D. Tang, *Anal. Chem.*, 2019, **91**, 4149–4156.
14 X. Pei, B. Zhang, J. Tang, B. Liu, W. Lai and D. Tang, *Anal. Chim. Acta*, 2013, **758**, 1–18.
15 B. Zhang, D. Tang, R. Goryacheva, R. Niessner and D. Knopp, *Chem. – Eur. J.*, 2013, **19**, 2496–2503.
16 E. Alipour, S. Norouzi and S. Moradi, *Anal. Methods*, 2021, **13**, 719–729.
17 S. Shahrokhian and S. Ranjbar, *ACS Sustainable Chem. Eng.*, 2019, **7**, 12760–12769.
18 Z. Chu, Y. Liu and W. Jin, *Biosens. Bioelectron.*, 2017, **96**, 17–25.
19 M. Busquets and J. Estelrich, *Drug Discovery Today*, 2020, **25**, 1431–1443.
20 B. Zhang, H. Ding, Q. Chen, T. Wang and K. Zhang, *Analyst*, 2019, **144**, 4858–4864.
21 J. Luo, T. Li and M. Yang, *Chin. Chem. Lett.*, 2020, **31**, 202–204.
22 D. Tang, J. Tang, B. Su, H. Chen, J. Huang and G. Chen, *Microchim. Acta*, 2010, **171**, 457–464.
23 J. Li, M. Shen and X. Shi, *ACS Appl. Bio Mater.*, 2020, **3**, 5590–5605.
24 C. Song, M. Shen, J. Rodrigues, S. Miganni, J. Majoral and X. Shi, *Coordination Chem. Rev.*, 2020, **421**, 213463.
25 Q. Li, J. Jing, F. Lou and D. Tang, *Sci. China: Chem.*, 2018, **61**, 750.
26 Z. Qiu, J. Shu and D. Tang, *Anal. Chem.*, 2017, **89**, 5152–5160.
27 T. Bertok, L. Lorencova, E. Chocholova, E. Jane, A. Vikartovska, P. Kasak and J. Tkac, *ChemElectroChem*, 2019, **6**, 989–1003.
28 K. Krukiewicz, *Electrochem. Commun.*, 2020, **116**, 106742.
29 B. Zhang, B. Liu, D. Tang, R. Niessner, G. Chen and D. Knopp, *Anal. Chem.*, 2012, **84**, 5392–5399.
30 Y. Lin, Q. Zhou, D. Tang, R. Niessner and D. Knopp, *Anal. Chem.*, 2017, **89**, 5637–5645.
31 J. Zhao, J. Du, J. Luo, S. Che and R. Yuan, *Sens. Actuators, B*, 2020, **311**, 127934.
32 L. Wang, B. Xing, X. Ren, X. Hu, H. Wang, D. Wu and Q. Wei, *Biosens. Bioelectron.*, 2020, **150**, 111910.
33 N. Ma, T. Zhang, T. Yan, X. Kuang, H. Wang, D. Wu and Q. Wei, *Biosens. Bioelectron.*, 2019, **143**, 111608.
34 D. Sun, X. Lin, J. Lu, P. Wei, Z. Luo, X. Lu, Z. Chen and L. Zhang, *Biosens. Bioelectron.*, 2019, **142**, 111578.
35 D. Sun, Z. Luo, J. Lu, S. Zhang, T. Che, Z. Chen and L. Zhang, *Biosens. Bioelectron.*, 2019, **134**, 49–56.
36 E. Ni, Y. Fang, F. Ma, G. Ge, J. Wu, Y. Wang, Y. Lin and H. Xie, *Anal. Methods*, 2020, **12**, 2914–2921.
37 G. Liu, M. Qi, Y. Zhang, C. Cao and E. Goldys, *Anal. Chim. Acta*, 2016, **909**, 1–8.
38 A. Peryaharuppan, R. Gandhiraman, M. Meyyappan and J. Koehne, *Anal. Chem.*, 2013, **85**, 3858–3863.

